Earthquakes and Structures, *Vol. 9, No. 3 (2015) 577-601*
DOI: http://dx.doi.org/10.12989/eas.2015.9.3.577

Reflection and refraction of magneto-thermoelastic plane wave at the pre-stressed liquid-solid interface in generalized thermoelasticity under three theories

Rajneesh Kakar[*1] and Shikha Kakar[2a]

[1] *Chotti Baradari, 163/1, Jalandhar, India*
[2] *Department of Electronics, SBBSIET, Padhiana, India*

(Received November 6, 2014, Revised January 3, 2015, Accepted January 7, 2015)

Abstract. The thermomagnetic effect on plane wave propagation at the liquid-solid interface with nonclassical thermoelasticity is investigated. It is assumed that liquid-solid half-space is under initial stress. Numerical computations are performed for the developed amplitude ratios of P, SV and thermal waves under Cattaneo-Lord-Shulman theory, Green-Lindsay theory and classical thermoelasticity. The system of developed equations is solved by the application of the MATLAB software at different angles of incidence for Green and Lindsay model. The effect of initial stress and magnetic field in the lower half-space are discussed and comparison is made in LS, GL and CT models of thermoelasticity. In the absence of magnetic field, the obtained results are in agreement with the same results obtained by the relevant authors. This study would be useful for magneto-thermoelastic acoustic device field.

Keywords: initial stress; reflection; refraction; relaxation time; temperature; magnetic field

1. Introduction

The study of acoustic wave behavior at the interface of magneto-thermoelastic solid and liquid media is a useful topic in acoustic non-destructive evaluation and acoustic device design. This problem has been investigated by many researchers for both viscous and non-viscous fluids and some useful solutions are found. Some of the related references are mentioned herein because it is not possible to embrace all of them. Chen *et al*. (2008) illustrated the reflection and transmission of plane waves in magneto-electro-elastic layered structures. Othman and Song (2008) proposed reflection of magneto-thermoelastic waves without initial stress. Zhang (2013) studied reflection and transmission of magneto-electro-elastic plane waves at the interface between solid and liquid media.

The heat propagation is considered to be infinitely large in the classical dynamical theory of thermoelasticity. This paradox is removed by the different generalizations of thermoelasticity such as Lord and Shulman (L-S) and Green and Lindsay (G-L) theories. Green and Lindsay theory

∗Corresponding author, Professor, E-mail: rajneesh.kakar@gmail.com
[a] HOD, E-mail: shikha_kakar@rediffmail.com

Copyright © 2015 Techno-Press, Ltd.
http://www.techno-press.org/journals/eas&subpage=7 ISSN: 2092-7614 (Print), 2092-7622 (Online)

(1973) included temperature rate among the constitutive variables and proposed theory of thermoelasticity in the context of classical Fourier law of heat conduction by considering center symmetry of body and removed the paradox of infinite thermal speed. Lord and Shulman (1967) proposed a generalized theory by introducing changing flux in Fourier's law of heat conduction and proposed finite speed for thermal vibrations. However, in many problems such as in nuclear reactors where steep heat gradients along with short time effects are involved, these theories don't give correct values. In context of these theories, Dey and Addy (1973) studied reflection of plane waves at a free surface under initial stresses. Sinha and Elsibai (1996) discussed thermoelastic reflection of waves at a solid half-space in the context of generalized theories of thermoelasticity. Sharma et al. (2003) investigated reflection of thermoelastic waves at the interface of a half-space by using thermoelastic theories. In last decade, considerable interest has been shown towards the phenomenon of magneto-electro-elastic plane wave propagation by many scientists; Wu *et al* (2007) discovered Lamb wave propagation in an infinite magneto-electro-elastic plate. Feng *et al* (2008) studied the Stoneley waves between two magneto-electro-elastic half planes by considering twenty five sets of magneto-electric interface conditions. Melkumyan (2007) investigated propagation of twelve surface waves in magneto-electro-elastic materials. Singh and Chakraborty (2013) studied reflection and refraction of thermoelastic plane waves at solid-liquid interface by considering three theories of thermoelasticity without considering magnetic parameter. However they took wrong parameter in their basic equations. Also, Kaur and Sharma (2012) discussed reflection and transmission of thermoelastic plane waves in the absence of magnetic field at liquid-solid interface. Sharma and Bhargava (2014) studied plane wave propagation at the interface of liquid-solid but they have not taken effect of magnetic field on plane thermoelastic waves. To the best knowledge of the authors, the reflection and refraction of magneto-thermoelastic plane wave at the interface between solid and liquid media under initial stress have not been investigated so far. This problem could be useful to design underwater acoustic device equipments. Therefore, authors have chosen engineering-oriented problem and it motivates the present study. The expression of reflection and refraction coefficients of magneto-thermoelastic plane wave in generalized theories of thermoelasticity is first formulated under boundary conditions and then computed numerically. The effect of initial stress, temperature and magnetic field upon the reflection and refraction coefficients of plane waves at liquid-solid interface are shown graphically.

2. Formulation of the problem

We consider a transversely isotropic, homogeneous elastic half space and non-viscous liquid half- space placed over it. Both the half-spaces are under initial tensile stress P along *X*-axis at absolute temperature T (Fig. 1). Further, thermoelastic medium is subjected to uniform magnetic field intensity $\mathrm{H}\left(0,0,\mathrm{H}_0\right)$ parallel to *Z*-axis. An elastic plane SV-wave (rotational wave), P-wave (dilatational wave) or thermal wave (dilatational wave) is incident in medium M_1 at the plane liquid-solid interface such that it is partially reflected as SV-wave (rotational wave) in medium M_1, one reflected P-wave (dilatational wave) in medium M_1, one reflected thermal wave (compressional wave) in medium M_1, one refracted P-wave (compressional wave) in medium M_2 and one reflected thermal wave (compressional wave) in medium M_2 as shown (Fig. 1).

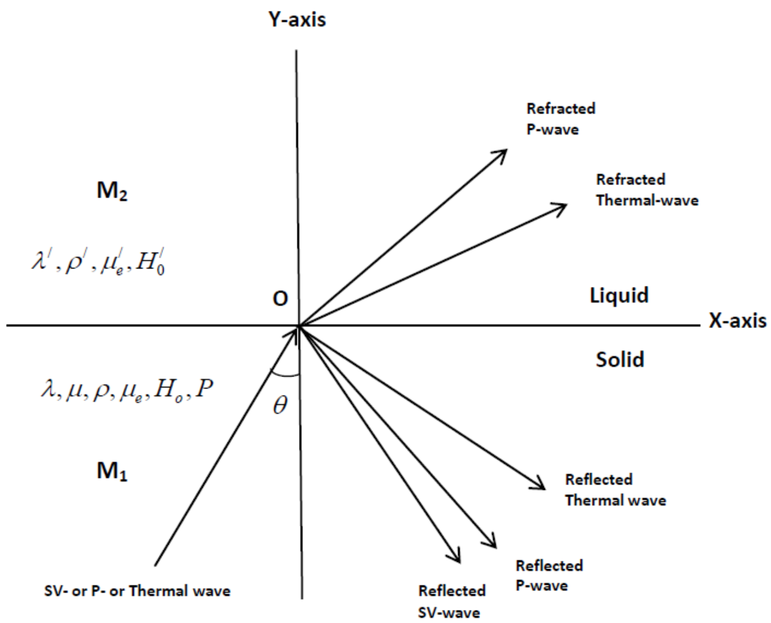

Fig. 1 Reflection and refraction of magneto-thermoelastic plane waves

3. Governing equations

The magnetic field is taken parallel to the *Z*-axis, therefore third *Z*-component ‘ w ’of the displacement vector and all other quantities are independent of *Z*. Following Lotfy (2011), the governing equations in the absence of all body forces are given by

Strain-displacement relations

$$e_{ij} = \frac{1}{2}(\mathrm{u}_{i.j} + \mathrm{u}_{j,\mathrm{i}}) \tag{1}$$

where, $\mathrm{u}_i = (u, v, 0)$ is the components of displacement vector.

Stress displacement relation

$$s_{ij} = \lambda\,\mathrm{e}\,\delta_{ij} + 2\mu e_{ij} - \gamma\left(1 + \tau\frac{\partial}{\partial t}\right)\mathrm{T}\delta_{ij}, \tag{2}$$

The modified heat conduction equation

$$\mathrm{K}\nabla^2\mathrm{T} = \rho c_v\left(\frac{\partial \mathrm{T}}{\partial t} + \tau_0\frac{\partial^2\mathrm{T}}{\partial t^2}\right) + \gamma\,\mathrm{T}_0\left(\frac{\partial^2 u}{\partial x\partial t} + \frac{\partial^2 v}{\partial y\partial t} + \tau_0\delta_{ij}\left[\frac{\partial^3 u}{\partial x\partial t^2} + \frac{\partial^3 v}{\partial y\partial t^2}\right]\right) \tag{3}$$

The components of Lorentz force

$$F_x = \mu_e(\mathrm{J}\times\mathrm{H})_x, \quad F_y = \mu_e(\mathrm{J}\times\mathrm{H})_y, \;\; F_z = 0 \tag{4}$$

The uniform magnetic field intensity $\mathrm{H}\left(0,0,\mathrm{H}_0\right)$ is parallel to *Z*-axis; it induces electric field E and magnetic field h. These variations in magnetic and electric fields are given by Maxwell's equations

$$\text{curl h} = \mathrm{J} + \frac{\partial \mathrm{D}}{\partial t} \tag{5}$$

$$\text{curl E} = -\frac{\partial \mathrm{B}}{\partial t} \tag{6}$$

$$\text{div B} = 0, \quad \text{div B} = 0, \quad \mathrm{B} = \mu_e \mathrm{H}, \quad \mathrm{D} = \varepsilon_e \mathrm{E} \tag{7}$$

$$\mathrm{E} = -\mu_e \left[\frac{\partial u}{\partial t} \times \mathrm{H} \right] \tag{8}$$

where $\frac{\partial u}{\partial t}$ is the particle velocity of the medium, and the influence of temperature gradient on J is also neglected. The steady-state deformed position is measured from dynamic displacement vector, which is assumed to be ignored.

The components of magnetic intensity vector in the medium

$$\mathrm{H}_x = \mathrm{H}_y = 0, \ \mathrm{H}_z = \mu_e[\mathrm{H}_0 + \mathrm{h(x,z,t)}] \tag{9}$$

$$\mathrm{J}_x = -\mathrm{H}_0 \frac{\partial e}{\partial y} + \mu_e \mathrm{H}_0 \varepsilon_e \frac{\partial^2 v}{\partial t^2}, \ \mathrm{J}_y = \mathrm{H}_0 \frac{\partial e}{\partial x} - \mu_e \mathrm{H}_0 \varepsilon_e \frac{\partial^2 u}{\partial t^2}, \ \mathrm{J}_z = 0 \tag{10}$$

From Eqs. (5)-(10) into Eq. (4) we obtain

$$F_x = \mu_e \mathrm{H}_0^2 \frac{\partial e}{\partial x} - \mu_e^2 \mathrm{H}_0^2 \varepsilon_e \frac{\partial^2 u}{\partial t^2}, \ \ F_y = \mu_e \mathrm{H}_0^2 \frac{\partial e}{\partial y} - \mu_e^2 \mathrm{H}_0^2 \varepsilon_e \frac{\partial^2 v}{\partial t^2}, \ \ F_z = 0 \tag{11}$$

where $\mathrm{h} = -\mathrm{H}_0(0,0,\mathrm{e})$

Following Biot [22], the dynamical equations of motion for the propagation of wave in two dimensions

$$\frac{\partial s_{xx}}{\partial x} + \frac{\partial s_{xy}}{\partial y} - P\frac{\partial \Omega}{\partial y} + F_x = \rho \frac{\partial^2 u}{\partial t^2} \tag{12}$$

$$\frac{\partial s_{xy}}{\partial x} + \frac{\partial s_{yy}}{\partial y} - P\frac{\partial \Omega}{\partial x} + F_y = \rho \frac{\partial^2 v}{\partial t^2} \tag{13}$$

where s_{xx}, s_{yy} and s_{xy} are incremental thermal stress components. The first two are principal stress components along *X*- and *Y*-axes, respectively and last one is shear stress component in the *X*-*Y* plane and *u*, *v* are the displacement components along *X* and *Y* directions respectively.

Following Biot [22], the stress-strain relations with incremental isotropy

$$s_{xx} = (\lambda + 2\mu + P)e_{xx} + (\lambda + P)e_{yy} + 2\mu e_{xx} - \gamma\left(\mathrm{T} + \tau\frac{\partial \mathrm{T}}{\partial x}\right) \tag{14}$$

$$s_{yy} = \lambda e_{xx} + (\lambda + 2\mu)e_{yy} - \gamma\left(\mathrm{T} + \tau\frac{\partial \mathrm{T}}{\partial x}\right) \tag{15}$$

$$s_{xy} = 2\mu e_{xy} \tag{16}$$

where

$$e_{xx} = \frac{\partial u}{\partial x}, \qquad e_{yy} = \frac{\partial v}{\partial x}, \qquad e_{xy} = \frac{1}{2}\left(\frac{\partial v}{\partial x} + \frac{\partial u}{\partial y}\right) \tag{17}$$

4. Solution of the problem

For lower half M_1

Using Eq. (11), Eqs. (14)-(17) in Eq. (12) and Eq. (13) we get

$$\left(\lambda + 2\mu + P\right)\frac{\partial^2 u}{\partial x^2} + \left(\lambda + \mu + \frac{P}{2}\right)\frac{\partial^2 v}{\partial x \partial y} + \left(\mu + \frac{P}{2}\right)\frac{\partial^2 u}{\partial^2 y} + \mu_e H_0^2\left(\frac{\partial^2 u}{\partial x^2} + \frac{\partial^2 v}{\partial x \partial y}\right) = \rho\frac{\partial^2 u}{\partial t^2} + \gamma\left(\frac{\partial \mathrm{T}}{\partial x} + \tau\frac{\partial^2 \mathrm{T}}{\partial t \partial x}\right) \tag{18}$$

$$\left(\lambda + 2\mu\right)\frac{\partial^2 v}{\partial y^2} + \left(\lambda + \mu + \frac{P}{2}\right)\frac{\partial^2 u}{\partial x \partial y} + \left(\mu - \frac{P}{2}\right)\frac{\partial^2 v}{\partial^2 x} + \mu_e H_0^2\left(\frac{\partial^2 u}{\partial x \partial y} + \frac{\partial^2 v}{\partial y^2}\right) = \rho\frac{\partial^2 v}{\partial t^2} + \gamma\left(\frac{\partial \mathrm{T}}{\partial y} + \tau\frac{\partial^2 \mathrm{T}}{\partial t \partial y}\right) \tag{19}$$

Eq. (18) and Eq. (19) can be solved by choosing potential functions ϕ and ψ as

$$u = \frac{\partial \phi}{\partial x} - \frac{\partial \psi}{\partial y} \text{ and } v = \frac{\partial \phi}{\partial x} + \frac{\partial \psi}{\partial y} \tag{20}$$

From Eqs. (18) and (20), we get

$$\nabla^2 \phi = \frac{\rho}{(\lambda + 2\mu + \mu_e H_0^2 + P)}\frac{\partial^2 \phi}{\partial t^2} + \frac{\gamma}{(\lambda + 2\mu + \mu_e H_0^2 + P)}\left(\mathrm{T} + \tau\frac{\partial \mathrm{T}}{\partial t}\right) \tag{21}$$

$$\nabla^2 \psi = \frac{\rho}{\left(\mu + \frac{P}{2}\right)}\frac{\partial^2 \psi}{\partial t^2} \tag{22}$$

From Eq. (19) and (20), we get

$$\nabla^2 \phi = \frac{\rho}{(\lambda + 2\mu + \mu_e H_0^2)}\frac{\partial^2 \phi}{\partial t^2} + \frac{\gamma}{(\lambda + 2\mu + \mu_e H_0^2)}\left(\mathrm{T} + \tau\frac{\partial \mathrm{T}}{\partial t}\right) \tag{23}$$

$$\nabla^2\psi = \frac{\rho}{\left(\mu - \frac{P}{2}\right)}\frac{\partial^2\psi}{\partial t^2} \tag{24}$$

Solution using Green and Lindsay's model

Eq. (21) and Eq. (23) represent magneto- thermo compression waves along *X*- axis and *Y*- axis respectively, whereas Eq. (22) and Eq. (24) represent magneto- thermo distortional waves along *X*- axis and *Y*- axis respectively. For initial stress along *X*- axis, the four Eqs. (21)-(24) by using Green and Lindsay's theory: $\tau \geq \tau_0 > 0,\ \ \delta_{ij} = 0,$ reduced to

$$\nabla^2\phi = \frac{1}{c_1^2}\frac{\partial^2\phi}{\partial t^2} + \frac{\gamma}{(\lambda + 2\mu + \mu_e H_0^2 + P)}\left(T + \tau\frac{\partial T}{\partial t}\right) \tag{25}$$

$$\nabla^2\psi = \frac{1}{c_2^2}\frac{\partial^2\psi}{\partial t^2} \tag{26}$$

where

$$c_1^2 = \frac{(\lambda + 2\mu + \mu_e H_0^2 + P)}{\rho} \text{ and } c_2^2 = \frac{\left(\mu - \frac{P}{2}\right)}{\rho} \tag{27}$$

c_1 is known as P-wave velocity and c_2 is called SV-wave velocity. Also, for P-wave $v = 0$ and for SV-wave $u = 0$.

Now, from Eqs. (3) and (20), we get

$$K\nabla^2\mathrm{T} = \rho c_v\left(\frac{\partial \mathrm{T}}{\partial t} + \tau_0\frac{\partial^2\mathrm{T}}{\partial t^2}\right) + \gamma\,\mathrm{T}_0\left[\frac{\partial}{\partial t}\left(\nabla^2\phi\right) + \delta_{ij}\tau_0\frac{\partial^2}{\partial t^2}\left(\nabla^2\phi\right)\right] \tag{28}$$

where, $\nabla^2 = \frac{\partial^2}{\partial x^2} + \frac{\partial^2}{\partial y^2}$

Using Green and Lindsay's theory: $\tau \geq \tau_0 > 0,\ \ \delta_{ij} = 0,$ Eq. (28) reduces as

$$K\nabla^2\mathrm{T} = \rho c_v\left(\frac{\partial \mathrm{T}}{\partial t} + \tau_0\frac{\partial^2\mathrm{T}}{\partial t^2}\right) + \gamma\,\mathrm{T}_0\left[\frac{\partial}{\partial t}\left(\nabla^2\phi\right)\right] \tag{29}$$

Eliminating T from Eq. (25) and Eq. (29), we get

$$\frac{\mathrm{K}}{\rho c_v}\nabla^4\phi - \left[\left(1 + \frac{\gamma^2\mathrm{T}_0}{\rho^2 c_v c_1^2}\right)\frac{\partial}{\partial t} + \left(\tau_0 + \frac{\gamma^2\mathrm{T}_0}{\rho^2 c_v c_1^2}\tau + \frac{\mathrm{K}}{c_v(\lambda + 2\mu + \mu_e H_0^2 + P)}\right)\frac{\partial^2}{\partial t^2}\right]\nabla^2\phi + \frac{\rho}{(\lambda + 2\mu + \mu_e H_0^2 + P)}\left(1 + \tau_0\frac{\partial}{\partial t}\right)\frac{\partial^3\phi}{\partial t^3} = 0 \tag{30}$$

Or

$$c_3^2\nabla^4\phi-\left[\left(1+\tau_{\mathrm{T}}\right)\frac{\partial}{\partial t}+\left(\tau_0+\tau_{\mathrm{T}}\tau+\frac{c_3^2}{c_1^2}\right)\frac{\partial^2}{\partial t^2}\right]\nabla^2\phi+\frac{1}{c_1^2}\left(1+\tau_0\frac{\partial}{\partial t}\right)\frac{\partial^3\phi}{\partial t^3}=0 \tag{31}$$

where, $c_3^2=\dfrac{\mathrm{K}}{\rho c_v}$ and $\tau_{\mathrm{T}}=\dfrac{\gamma^2\,\mathrm{T}_0}{\rho^2 c_v c_1^2}$ is thermoelastic coupling constant in medium M_1.

The solution of ϕ , ψ and T can be obtained in the following form

$$\phi=\mathrm{A}(y)\exp[i\{kx-ct\}] \tag{32}$$

$$\psi=\mathrm{B}(y)\exp[i\{kx-ct\}] \tag{33}$$

$$\mathrm{T}=C(y)\exp[i\{kx-ct\}] \tag{34}$$

where, k is wave number, ω is angular frequency and $c=\dfrac{\omega}{k}$ phase velocity.

Eq. (32) should satisfy Eq. (31) because Eq. (32) is a solution of Eq. (31), so substituting Eq. (32) in Eq. (31) we get

$$\begin{aligned}&\frac{d^4\mathrm{A}}{dy^4}+\left[-2k^2+\frac{k^2c^2}{c_3^2}\left(\tau_0+\tau_{\mathrm{T}}\tau+\frac{c_3^2}{c_1^2}\right)+\frac{ikc}{c_3^2}\left(1+\tau_{\mathrm{T}}\right)\right]\frac{d^2\mathrm{A}}{dy^2}\\&+\left[k^4-\frac{k^4c^2}{c_3^2}\left(\tau_0+\tau_{\mathrm{T}}\tau+\frac{c_3^2}{c_1^2}\right)+\frac{ik^3c^2}{c_1^2c_3^2}\left((1-ikc\tau_0\right)-\frac{ikc_1^2}{c^2}\left(1+\tau_{\mathrm{T}}\right)\right]\mathrm{A}=0\end{aligned} \tag{35}$$

The solution of Eq. (35) will contain four values of $\mathrm{A}(y)$, therefore Eq. (32) becomes

$$\phi=\begin{bmatrix}\alpha_1\exp\left(ik\xi_1 y\right)+\alpha_2\exp\left(-ik\xi_1 y\right)\\+\alpha_3\exp\left(ik\xi_2 y\right)+\alpha_4\exp\left(-ik\xi_2 y\right)\end{bmatrix}\exp[i\{kx-ct\}] \tag{36}$$

where, $\xi_1=\sqrt{c^2\delta_1^2-1}$, $\xi_2=\sqrt{c^2\delta_2^2-1}$

$$\begin{aligned}&\delta_1,\delta_2=\sqrt{\frac{1}{2c_1^2c_3^2}\left[\left\{c_1^2\left(\tau_0+\tau_{\mathrm{T}}\tau\right)+c_3^2+\frac{i(1+\tau_{\mathrm{T}})c_1^2}{\omega}\right\}\pm\sqrt{L}\right]},\\&L=\left[c_1^2\left(\tau_0+\tau_{\mathrm{T}}\tau\right)+c_3^2+\frac{i(1+\tau_{\mathrm{T}})c_1^2}{\omega}\right]^2-\frac{4i\left(1-i\omega\tau_0\right)c_1^2c_3^2}{\omega}\end{aligned} \tag{37}$$

From Eq. (33) and Eq. (26), we get

$$\frac{d^2\mathrm{B}}{dy^2}+k^2\left(\frac{c^2}{c_2^2}-1\right)\mathrm{B}=0 \tag{38}$$

The solution of Eq. (38) will contain four values of $\mathrm{B}(y)$, therefore Eq. (33) can be written as

$$\psi=\left[\alpha_5\exp\left(ik\xi_3 y\right)+\alpha_6\exp\left(-ik\xi_3 y\right)\right]\exp[i\{kx-ct\}] \tag{39}$$

where

$$\xi_3=\sqrt{\frac{c^2}{c_2^2}-1} \tag{40}$$

Here α_1 represent the amplitude of incident thermal wave ,α_2 represent the amplitude of reflected thermal wave, α_3 represent the amplitude of incident P- wave ,α_4 represent the amplitude of reflected P-wav α_5 represent the amplitude of incident SV-wave and α_6 represent the amplitude of reflected SV-wave respectively.

Substituting Eq. (36) and Eq. (34) in Eq. (25), we get the values of $C(y)$ and using that value of $C(y)$ in Eq. (34), we get

$$\mathrm{T}=\frac{\rho}{\varsigma\gamma}\begin{bmatrix} d\left\{\alpha_1\exp\left(ik\xi_1 y\right)+\alpha_2\exp\left(-ik\xi_1 y\right)\right\} \\ +f\left\{\alpha_3\exp\left(ik\xi_2 y\right)+\alpha_4\exp\left(-ik\xi_2 y\right)\right\}\end{bmatrix}\exp[i\{kx-ct\}] \tag{41}$$

where, $\varsigma=(1-i\omega\tau)$, $d=\omega^2(1-\delta_2\,\mathrm{c}_1^2)$ and $f=\omega^2(1-\delta_1\,\mathrm{c}_1^2)$

For upper half M_2

Using equation (11), equations (14)-(17) in equation (12) and equation (13) we get

$$\lambda'\frac{\partial^2 u'}{\partial x^2}+\lambda'\frac{\partial^2 v'}{\partial x\partial y}+\frac{\partial^2 u'}{\partial^2 y}+\mu_e' H_0'^2\left(\frac{\partial^2 u'}{\partial x^2}+\frac{\partial^2 v'}{\partial x\partial y}\right)=\rho'\frac{\partial^2 u'}{\partial t^2}+\gamma'\left(\frac{\partial \mathrm{T}'}{\partial x}+\tau'\frac{\partial^2 \mathrm{T}'}{\partial t\partial x}\right) \tag{42}$$

$$\lambda'\frac{\partial^2 v'}{\partial y^2}+\lambda'\frac{\partial^2 u'}{\partial x\partial y}+\frac{\partial^2 v'}{\partial^2 x}+\mu_e' H_0'^2\left(\frac{\partial^2 u'}{\partial x\partial y}+\frac{\partial^2 v'}{\partial y^2}\right)=\rho'\frac{\partial^2 v'}{\partial t^2}+\gamma'\left(\frac{\partial \mathrm{T}'}{\partial x}+\tau'\frac{\partial^2 \mathrm{T}'}{\partial t\partial y}\right) \tag{43}$$

Similarly, Eq. (3) for upper half M_2 can be written as

$$K'\nabla^2\mathrm{T}'=\rho' c_v'\left(\frac{\partial \mathrm{T}'}{\partial t}+\tau_0'\frac{\partial^2 \mathrm{T}'}{\partial t^2}\right)+\gamma'\mathrm{T}_0'\left[\frac{\partial}{\partial t}\left(\frac{\partial u'}{\partial x}+\frac{\partial v'}{\partial y}\right)\right] \tag{44}$$

Here, $\lambda',\mu_e',H_0',\rho',\gamma',\tau',K',c_v',.\mathrm{T}_0',\tau_0'$ are the quantities for the upper half medium M_2 as defined for lower half medium M_1

$$\text{Let } u'=\frac{\partial\phi'}{\partial x} \text{ and } v'=\frac{\partial\phi'}{\partial y} \tag{45}$$

we get

$$\nabla^2\phi'=\frac{1}{c_1'^2}\frac{\partial^2\phi'}{\partial t^2}+\frac{\gamma'}{\rho' c_1'^2}\left(\mathrm{T}'+\tau'\frac{\partial \mathrm{T}'}{\partial t}\right) \tag{46}$$

$$K'\nabla^2\mathrm{T}'=\rho' c'_v\left(\frac{\partial \mathrm{T}'}{\partial t}+\tau'_0\frac{\partial^2\mathrm{T}'}{\partial t^2}\right)+\gamma'\mathrm{T}'_0\left[\frac{\partial}{\partial t}\left(\nabla^2\phi'\right)\right] \tag{47}$$

where, $c_1'^2=\dfrac{(\lambda'+\mu'_e H_0'^2)}{\rho'}$

The solutions of Eq. (46) and Eq. (47) can be obtained in the same manner as in lower half-space medium M_1 as given below

$$\phi'=\left[\alpha'_2\exp\left(ik\xi'_1 y\right)+\alpha'_4\exp\left(ik\xi'_2 y\right)\right]\exp[i\{kx-ct\}] \tag{48}$$

$$\mathrm{T}'=\frac{\rho'}{\varsigma'\gamma'}\left[d'\alpha'_2\exp\left(ik\xi'_1 y\right)+e'\alpha'_4\exp\left(ik\xi'_2 y\right)\right]\exp[i\{kx-ct\}] \tag{49}$$

where

$$\xi'_1=\sqrt{c^2\delta_1'^2-1},\ \xi'_2=\sqrt{c^2\delta'_2-1},$$

$$\delta'_1,\delta'_2=\sqrt{\frac{1}{2c_1'^2c_3'^2}\left[\left\{c_1'^2\left(\tau'_0+\tau'_\mathrm{T}\tau'\right)+c_3'^2+\frac{i(1+\tau'_\mathrm{T})c_1'^2}{\omega}\right\}\pm\sqrt{L'}\right]},$$

$$L'=\left[c_1'^2\left(\tau'_0+\tau'_\mathrm{T}\tau'\right)+c_3'^2+\frac{i(1+\tau'_\mathrm{T})c_1'^2}{\omega}\right]^2-\frac{4i\left(1-i\omega\tau'_0\right)c_1'^2c_3'^2}{\omega},\ \varsigma'=(1-i\omega\tau'), \tag{50}$$

$$d'=\omega^2(1-\delta'_2\,\mathrm{c}_1'^2)\ \text{and}\ e'=\omega^2(1-\delta'_1\,\mathrm{c}_1'^2)$$

Here α'_2 and α'_4 are the amplitude of refracted thermal wave and refracted P-wave respectively.

Solution using Lord and Shulman's model

In this model, $\tau=0,\ \tau_0>0,\ \delta_{ij}=1$, putting this condition in the Eqs. (12-17) as for the Green and Lindsay's model, we get the solution for $\phi,\psi,\mathrm{T},\phi'$ and T' in the same manner in the Eqs. (36), (39), (41), (48) and (49) respectively with

$$\xi_1=\sqrt{c^2\delta_1^2-1},\ \xi_2=\sqrt{c^2\delta_2^2-1},\ \xi_3=\sqrt{\frac{c^2}{c_2^2}-1},\ \xi'_1=\sqrt{c^2\delta_1'^2-1},\ \xi'_2=\sqrt{c^2\delta'_2-1},\ \varsigma=\varsigma'=1$$

where

$$\delta_1,\delta_2=\sqrt{\frac{1}{2c_1^2c_3^2}\left[\left\{c_1^2+c_3^2+\frac{i(1+\tau_\mathrm{T})c_1^2}{\omega}\right\}\pm\sqrt{L}\right]},\ L=\left[c_1^2+c_3^2+\frac{i(1+\tau_\mathrm{T})c_1^2}{\omega}\right]^2-\frac{4ic_1^2c_3^2}{\omega},$$

$$\delta'_1,\delta'_2=\sqrt{\frac{1}{2c_1'^2c_3'^2}\left[\left\{c_1'^2+c_3'^2+\frac{i(1+\tau'_\mathrm{T})c_1'^2}{\omega}\right\}\pm\sqrt{L'}\right]}, \tag{51}$$

$$L'=\left[c_1'^2+c_3'^2+\frac{i(1+\tau'_\mathrm{T})c_1'^2}{\omega}\right]^2-\frac{4ic_1'^2c_3'^2}{\omega}$$

Solution using Classical Dynamical model

In this model, $\tau = \tau_0 = 0, \delta_{ij} = 0$, putting this condition in the Eqs. (12)-(17) as for the classical dynamical model, we get the solution for $\phi, \psi, \mathrm{T}, \phi'$ and T' in the same manner in the Eqs. (36), (39), (41), (48) and (49) respectively with

$$\xi_1 = \sqrt{c^2\delta_1^2 - 1},\ \xi_2 = \sqrt{c^2\delta_2^2 - 1},\ \xi_3 = \sqrt{\frac{c^2}{c_2^2} - 1},\ \xi_1' = \sqrt{c^2\delta_1'^2 - 1},\ \xi_2' = \sqrt{c^2\delta_2' - 1},\ \varsigma = \varsigma' = 1$$

where

$$\delta_1, \delta_2 = \sqrt{\frac{1}{2c_1^2c_3^2}\left[\left\{c_1^2 + c_3^2 + \frac{i(1+\tau_{\mathrm{T}})c_1^2}{\omega}\right\} \pm \sqrt{L}\right]},\ L = \left[c_1^2 + c_3^2 + \frac{i(1+\tau_{\mathrm{T}})c_1^2}{\omega}\right]^2 - \frac{4ic_1^2c_3^2}{\omega},$$

$$\delta_1', \delta_2' = \sqrt{\frac{1}{2c_1'^2c_3'^2}\left[\left\{c_1'^2 + c_3'^2 + \frac{i(1+\tau_{\mathrm{T}}')c_1'^2}{\omega}\right\} \pm \sqrt{L'}\right]}, \tag{52}$$

$$L' = \left[c_1'^2 + c_3'^2 + \frac{i(1+\tau_{\mathrm{T}}')c_1'^2}{\omega}\right]^2 - \frac{4ic_1'^2c_3'^2}{\omega}$$

5. Boundary conditions and Reflection and refraction coefficients

The initial conditions are supplemented by the following boundary conditions:

Continuity condition for normal displacement at $Y = 0$

$$v = v' \tag{53a}$$

Continuity condition for tangential displacement at $Y = 0$

$$u = 0 \tag{53b}$$

Continuity condition for normal initial stress at $Y = 0$

$$\nabla f_y = \nabla f_y' \tag{53c}$$

Continuity condition for tangential initial stress at $Y = 0$

$$\nabla f_x = \nabla f_x' \tag{53d}$$

Continuity condition for temperature at $Y = 0$

$$T = T' \tag{53e}$$

First boundary condition (53a) gives

$$\frac{\partial\phi}{\partial y} + \frac{\partial\psi}{\partial x} = \frac{\partial\phi'}{\partial y} \tag{54}$$

Introducing Eq. (36), Eq. (39) and Eq. (48) in Eq. (54) for medium M_1 and corresponding equations for the medium M_2, we get

$$\xi_1\alpha_1 - \xi_1\alpha_2 + \xi_2\alpha_3 - \xi_2\alpha_4 + \alpha_5 + \alpha_6 - \xi_1'\alpha_2' - \xi_2'\alpha_4' = 0 \tag{55}$$

Second boundary condition (53b) gives

$$\frac{\partial\phi}{\partial y} - \frac{\partial\psi}{\partial x} = 0 \tag{56}$$

Introducing Eq. (36) and Eq. (39) in Eq. (56), we get

$$\alpha_1 + \alpha_2 + \alpha_3 + \alpha_4 - \xi_3\alpha_3 + \xi_3\alpha_6 = 0 \tag{57}$$

Third boundary condition (53c) gives

$$s_{yy} = s_{yy}' \tag{58}$$

Introducing Eqs. (14)-(17) in Eq. (58) for medium M_1 and corresponding equations for the medium M_2, we get from Eq. (20) and Eq. (46)

$$\begin{aligned}\left(\lambda + \mu_e H_0^2\right)\left(\frac{\partial^2\phi}{\partial x^2} + \frac{\partial^2\phi}{\partial y^2}\right) + 2\mu\frac{\partial^2\phi}{\partial y^2} + 2\mu\frac{\partial^2\psi}{\partial x\partial y} - \gamma\left(\mathrm{T} + \tau\frac{\partial \mathrm{T}}{\partial t}\right) \\ = \left(\lambda' + \mu_e' H_0'^2\right)\left(\frac{\partial^2\phi'}{\partial x^2} + \frac{\partial^2\phi'}{\partial y^2}\right) - \gamma'\left(\mathrm{T}' + \tau'\frac{\partial \mathrm{T}'}{\partial t}\right)\end{aligned} \tag{59}$$

Introducing Eq. (36), Eq. (39), Eq. (41) and Eq. (48) in Eq. (59), we get

$$\begin{aligned}&\left[-(2+\beta) + c^2\left(\frac{1}{c_2^2} - \beta\delta_2^2\right)\right](\alpha_1 + \alpha_2) + \left[-(2+\beta) + c^2\left(\frac{1}{c_2^2} - \beta\delta_1^2\right)\right](\alpha_3 + \alpha_4) \\ &+ (2+\beta)\xi_3(\alpha_5 - \alpha_6) - \bar{\rho}\left(1 + \xi_3^2\right)(\alpha_2' + \alpha_4') = 0\end{aligned} \tag{60}$$

where, $\bar{\rho} = \dfrac{\rho'}{\rho}$ and $\beta = \dfrac{P}{\rho c_2^2}$.

Fourth boundary condition (53d) gives

$$s_{xy} + Pe_{xy} = 0 \tag{61}$$

Introducing Eqs. (14)-(17), Eq. (20), Eq. (36) and Eq. (39) in Eq. (61), we get

$$\xi_1(\alpha_1 - \alpha_2) + \xi_2(\alpha_3 - \alpha_4) - \frac{1}{2}\left(\xi_3^2 - 1\right)(\alpha_5 + \alpha_6) = 0 \tag{62}$$

Introducing Eq. (36), Eq. (41) and Eq. (49) in Eq. (53e) for medium M_1 and corresponding equations for the medium M_2, we get

$$\left(1 - \delta_2^2 c_1^2\right)(\alpha_1 + \alpha_2) + \left(1 - \delta_1^2 c_1^2\right)(\alpha_3 + \alpha_4) - \frac{\bar{\rho}}{\varsigma^*\bar{\gamma}}\left[\left(1 - \delta_2'^2 c_1'^2\right)\alpha_2' + \left(1 - \delta_1'^2 c_1'^2\right)\alpha_4'\right] = 0 \tag{63}$$

where, $\overline{\gamma} = \dfrac{\gamma'}{\gamma}$ and $\varsigma^* = \dfrac{\varsigma'}{\varsigma}$.

Generalizing, we obtain a system of five non-homogeneous equations for a magneto thermoelastic plane wave incident

$$\sum_{j=1}^{5} c_{ij} R_j = q_i \qquad \text{(where } j\text{=1,2. . .5)} \tag{64}$$

$R_j = |R_j|$ are the amplitudes ratios of reflected thermal, reflected P-, reflected SV-waves and refracted thermal, refracted P-waves to that of incident wave respectively. The coefficients q_i on the right side of the Eq. (64) are given by:

For incident P-wave:

We put $c = \delta_1^{-1} \operatorname{cosec}\theta$ and $\alpha_1 = \alpha_5 = 0$.

$$q_1 = c_{12},\ q_2 = -c_{22},\ q_3 = -c_{32},\ q_4 = c_{42},\ q_5 = -c_{52},\ R_1 = \frac{\alpha_2}{\alpha_3},\quad R_2 = \frac{\alpha_4}{\alpha_3},\ R_3 = \frac{\alpha_6}{\alpha_3},$$
$$R_4 = \frac{\alpha_2'}{\alpha_3},\ R_5 = \frac{\alpha_4'}{\alpha_3}. \tag{65a}$$

For incident SV-wave:

We put $c = \delta_2^{-1} \operatorname{cosec}\theta$ and $\alpha_3 = \alpha_5 = 0$.

$$q_1 = -c_{13},\ q_2 = c_{23},\ q_3 = c_{33},\ q_4 = -c_{43},\ q_5 = c_{53},\ R_1 = \frac{\alpha_2}{\alpha_5},\quad R_2 = \frac{\alpha_4}{\alpha_5},\ R_3 = \frac{\alpha_6}{\alpha_5},$$
$$R_4 = \frac{\alpha_2'}{\alpha_5},\ R_5 = \frac{\alpha_4'}{\alpha_5}. \tag{65b}$$

For incident thermal wave:

We put $c = c_2 \operatorname{cosec}\theta$ and $\alpha_1 = \alpha_3 = 0$.

$$q_1 = c_{11},\ q_2 = -c_{21},\ q_3 = -c_{31},\ q_4 = c_{41},\ q_5 = -c_{51},\ R_1 = \frac{\alpha_2}{\alpha_1},\quad R_2 = \frac{\alpha_4}{\alpha_1},\ R_3 = \frac{\alpha_6}{\alpha_1},$$
$$R_4 = \frac{\alpha_2'}{\alpha_1},\ R_5 = \frac{\alpha_4'}{\alpha_1}. \tag{65c}$$

where

$$c_{11} = -\xi_1, c_{12} = -\xi_2, c_{13} = 1, c_{14} = -\xi_1', c_{15} = -\xi_2',\ c_{21} = 1, \mathrm{c}_{22}\, 1, \mathrm{c}_{23} = \xi_3, \mathrm{c}_{24} = 0, \mathrm{c}_{25} = 0, \tag{66}$$

$$c_{31}=\left[-\left(2+\beta\right)+c^2\left(\frac{1}{c_2^2}-\beta\delta_1^2\right)\right],c_{32}=\left[-\left(2+\beta\right)+c^2\left(\frac{1}{c_2^2}-\beta\delta_2^2\right)\right],c_{33}=-(2+\beta)\xi_3,$$

$$c_{34}=-\bar{\rho}\left(1+\xi_3^2\right),c_{35}=-\bar{\rho}\left(1+\xi_3^2\right),c_{41}=-\xi_1,c_{42}=-\xi_2,c_{43}=-\frac{1}{2}\left(\xi_3^2-1\right),c_{44}=0,c_{45}=0,$$

$$c_{51}=\left(1-\delta_2^2c_1^2\right),c_{52}=\left(1-\delta_1^2c_1^2\right),c_{53}=0,c_{54}=-\frac{\bar{\rho}}{\varsigma^*\bar{\gamma}}\left(1-\delta_2'c_1'^2\right),c_{55}=-\frac{\bar{\rho}}{\varsigma^*\bar{\gamma}}\left(1-\delta_2'^2c_1'^2\right).$$

For Lord and Shulman's model and Classical Dynamical model the matrix elements are

$$c_{11}=-\xi_1,c_{12}=-\xi_2,c_{13}=1,c_{14}=-\xi_1',c_{15}=-\xi_2',\ c_{21}=1,\mathrm{c}_{22}1,\mathrm{c}_{23}=\xi_3,\mathrm{c}_{24}=0,\mathrm{c}_{25}=0,$$

$$c_{31}=\left[-\left(2+\beta\right)+c^2\left(\frac{1}{c_2^2}-\beta\delta_1^2\right)\right],c_{32}=\left[-\left(2+\beta\right)+c^2\left(\frac{1}{c_2^2}-\beta\delta_2^2\right)\right],c_{33}=-(2+\beta)\xi_3,$$

$$c_{34}=-\bar{\rho}\left(1+\xi_3^2\right),c_{35}=-\bar{\rho}\left(1+\xi_3^2\right),c_{41}=-\xi_1,c_{42}=-\xi_2,c_{43}=-\frac{1}{2}\left(\xi_3^2-1\right),c_{44}=0,c_{45}=0, \tag{67}$$

$$c_{51}=\left(1-\delta_2^2c_1^2\right),c_{52}=\left(1-\delta_1^2c_1^2\right),c_{53}=0,c_{54}=-\frac{\bar{\rho}}{\bar{\gamma}}\left(1-\delta_2'c_1'^2\right),c_{55}=-\frac{\bar{\rho}}{\bar{\gamma}}\left(1-\delta_2'^2c_1'^2\right).$$

Eq. (64) can be written in terms of (5×5) matrix

$$\begin{bmatrix} c_{11} & c_{12} & c_{13} & c_{14} & c_{15} \\ c_{21} & c_{22} & c_{23} & c_{24} & c_{25} \\ c_{31} & c_{32} & c_{33} & c_{34} & c_{35} \\ c_{41} & c_{42} & c_{43} & c_{44} & c_{45} \\ c_{51} & c_{52} & c_{53} & c_{54} & c_{55} \end{bmatrix}\times\begin{bmatrix} R_1 \\ R_2 \\ R_3 \\ R_4 \\ R_5 \end{bmatrix}=\begin{bmatrix} q_1 \\ q_2 \\ q_3 \\ q_4 \\ q_5 \end{bmatrix} \tag{68}$$

6. Numerical analysis and discussion

From the above theory we conclude that the amplitude ratios $|R_i|$ depend on the incident angle of the incident wave. In order to study in greater detail, the dependence of these amplitude coefficients stress and magnetic parameter together with the incident angle, we compute the amplitude ratios. We have taken following material constants for water-cadmium composite (Table 1). For the values of relevant physical constants (Table 1), the system of Eq. (68) is solved for reflection and refraction coefficients by the application of the MATLAB software at different angles of incidence varying from 0° to 90° for Lord and Shulman's model, Green and Lindsay's model and classical thermoelasticity. Various graphs are plotted for Lord and Shulman's model, Green and Lindsay's model and classical thermoelasticity using a particular value of initial stress parameter and in second step, the curves are plotted for different values of initial stress parameters and magnetic parameters using Green and Lindsay's model. In the following graphs the results are

Table 1 Material Properties

Cadmium		Water	
ρ	$7.996\times10^{3}kg.m^{-3}$	ρ'	$1000kg/m^{3}$
λ	$4.048\times10^{12}N.m^{-2}$	λ'	$2\times10^{10}N/m^{2}$
α_t	$21\times10^{-6}K^{-1}$	α'_t	$69\times10^{-6}K^{-1}$
$\mu_e H_0^2$	$1.24\times10^{9}N/m^{2}$	$\mu'_e H_0'^2$	$1\times10^{9}N/m^{2}$
K	$96.6W\ m^{-1}.K^{-1}$	K′	$0.6\ Wm^{-1}K^{-1}$
c_v	$233J.kg^{-1}.K^{-1}$	c'_v	$4187\ Jkg^{-1}\ K^{-1}$
μ	$1.89\times10^{10}N/m^{2}$	μ'	$2\times10^{10}\ N/m^{2}$
$\bar{\gamma}$	0.96	$\bar{\gamma}$	0.96
$\bar{\rho}$	0.45	$\bar{\rho}$	0.45
T_0	$300K$	T_0	$300K$
ω	$7.5\times10^{13}s^{-1}$	ω	$7.5\times10^{13}s^{-1}$

shown with thermal wave incidence. To evaluate, we have introduced the initial stress parameter $a=\dfrac{P}{2\mu}$ in dimensionless form to calculate the matrix elements c_{ij} (in Appendix).

Here, ω is the angular frequency of magneto-thermoelastic waves. We have taken scale 10^{-1} to plot graphs and τ_0 and τ'_0 are of the same order i.e. 1.4 times approximately of τ and τ' (in Appendix). The subscript 'T' with reflection and refraction coefficients (R_i) is used to represent the tensile stress and subscript 'C' with reflection and refraction coefficients (R_i) represent compressive stress respectively.

Comparison among models

The comparison of different models with thermal wave incidence is shown in Figs. 2-5. The analysis of amplitude ratios for reflection and refraction coefficients when thermal wave is incident have been compared in Figs. 2-5, the initial stress parameter is taken *a*=+0.3 (tensile) and *a*=-0.3 (compressional). In Fig. 2, the analysis of amplitude ratio of reflected (a) Thermal wave $|R_T(1)|$, (b) P wave $|R_T(2)|$ and (c) SV wave $|R_T(3)|$ with incident angle for magneto-thermoelastic wave with tensile stress (*a*=0.3) constant value of magnetic parameter for incident thermal wave is shown and comparison among three models is made. We observe that the nature of analysis of reflection coefficients is almost similar in nature for all models of thermoelasticity. From Fig. 2, we observe that there is decrement of reflected thermal wave amplitude ratios with the increment in the incident angle. Further, the amplitude gradually decreases for the thermal wave reflection in Fig. 2(a). In Fig. 2(b), the reflection coefficient of P wave shows minima at θ=37° and θ=32° respectively in GL and LS model, while the amplitude ratio gradually decreases in CT model for P- wave reflection. In Fig. 2(c), reflection coefficient of SV wave in the LS model shows two maxima at θ=30° and θ=55°, maxima at θ=65° in the GL and maxima at θ=35° in the

CT model.

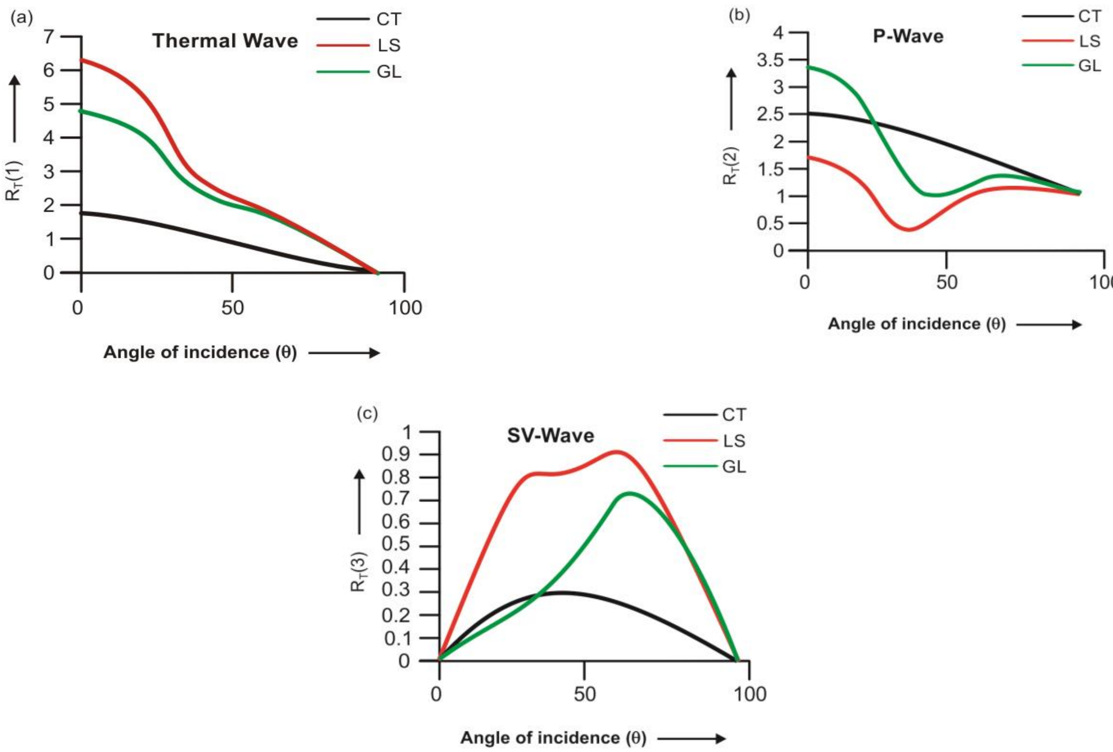

Fig. 2 Comparison among models: analysis of amplitude ratio of reflected (a) Thermal wave $|R_T(1)|$, P wave $|R_T(2)|$ and (c) SV wave $|R_T(3)|$ with incident angle under magnetic field with tensile stress (a=0.3) for incident thermal wave

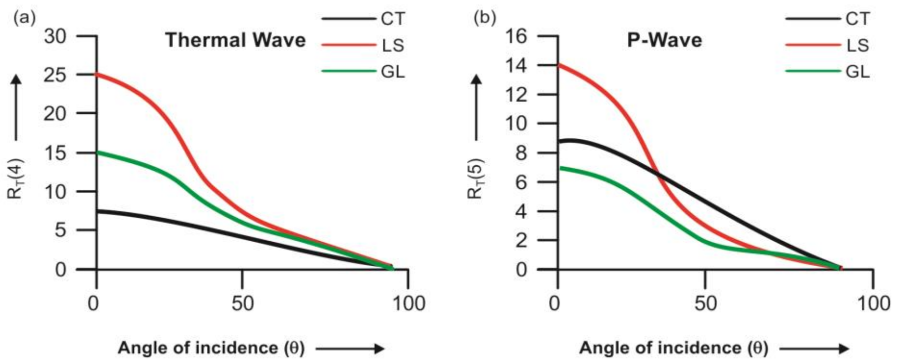

Fig. 3 Comparison among models: analysis of amplitude ratio of refracted (a) Thermal wave $|R_T(4)|$ and (b) P wave $|R_T(5)|$ with incident angle under magnetic field with tensile stress (a=0.3) in for incident thermal wave

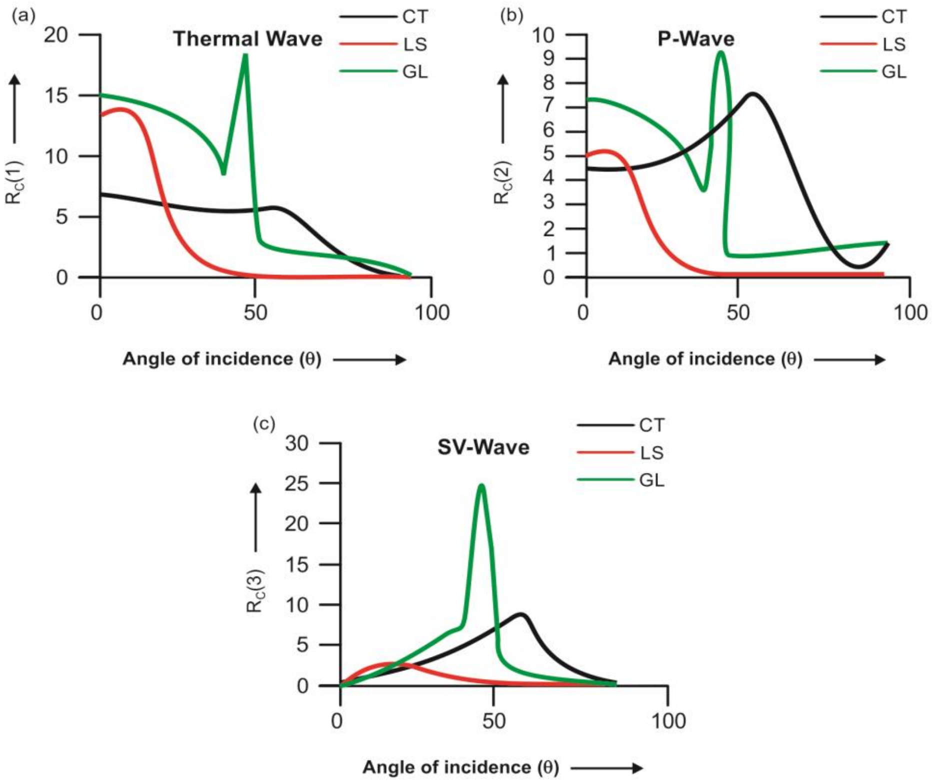

Fig. 4 Comparison among models: analysis of amplitude ratio of reflected (a) Thermal wave $|R_C(1)|$, (b) P wave $|R_C(2)|$ and (c) SV wave $|R_C(3)|$ with incident angle under compressional stress (a=-0.3) for incident thermal wave

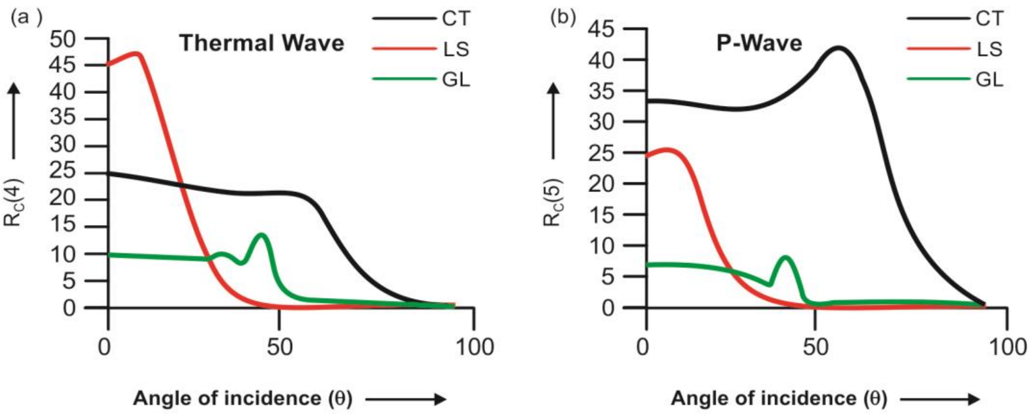

Fig. 5 Comparison among models: analysis of amplitude ratio of refracted (a) Thermal wave $|R_C(4)|$ and (b) P wave $|R_C(5)|$ with incident angle under compressional initial stress (a=-0.3) for incident thermal wave

Fig. 3 shows the analysis of amplitude ratio of refracted (a) Thermal wave $|R_T(4)|$ and (b) P wave $|R_T(5)|$ with incident angle under magnetic field with tensile stress (*a*=0.3) in for incident thermal wave and comparison among three models is made. Fig. 3(a) and 3(b) shows the amplitude ratios of the refracted waves decrease slowly for L-S, GL and CT models. Fig. 4 shows the analysis of amplitude ratio of reflected (a) Thermal wave $|R_C(1)|$, (b) P wave $|R_C(2)|$ and (c) SV wave $|R_C(3)|$ with incident angle under compressional stress (*a*=-0.3) and constant magnetic parameter for incident thermal wave and comparison among three models is made. Moreover, the nature of analysis of reflection coefficients is almost similar in nature for all the models of thermoelasticity under compressional stress. We observe that Fig. 4(a)-4(b) represent the

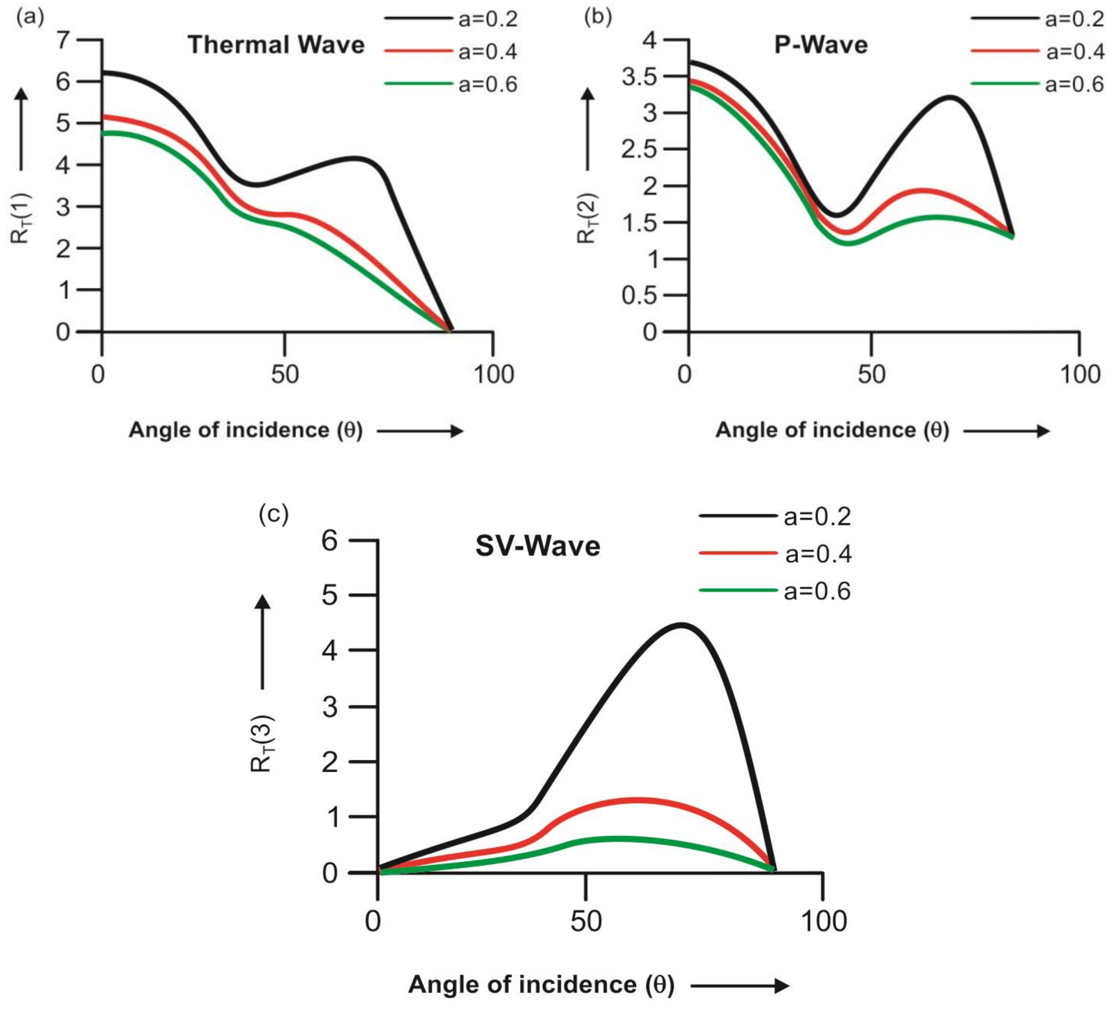

Fig. 6 Analysis of amplitude ratio of reflected (a) Thermal wave $|R_T(1)|$, P wave $|R_T(2)|$ and (c) SV wave $|R_T(3)|$ with incident angle under tensile stresses for GL model for incident thermal wave

amplitude ratios of reflected thermal and P waves, in this there are minima and maxima at θ=40° and θ=45° for GL model, while maxima at θ=60° for CT model. The reflection coefficient of SV wave in the GL model shows maxima at θ=40° and maxima at θ=60° in CT model. It is observed that the amplitude ratio falls sharply in LS model. Fig. 5 shows the analysis of amplitude ratio of refracted (a) Thermal wave $|R_C(4)|$ and (b) P wave $|R_C(5)|$ with incident angle under compressional initial stress (*a*=-0.3) and constant magnetic field for incident thermal wave and comparison among three models is made. In Fig. 5(a)-5(b), the refracted amplitude ratio falls sharply for 10°≤θ≤50° in LS model, maxima at θ=40° in GL model and refracted ratio falls gradually for CT model. On observing all the graphs under tensile or compressional stresses in three different models of generalized thermoelasticity, there is no doubt that reflection and refraction coefficients are totally dependent on magnetic field, initial stress and angle of incident of the magneto-thermoelastic wave.

Effect of initial stress

In Figs. 6-9 (when thermal wave is incident), the analysis of amplitude ratios with the incident angle been compared for different values of initial stress (tensile and compressional) at constant magnetic parameters by taking GL model as sample. In Fig. 6(a), there is a decrease in amplitude ratio up to θ=45° and with the increase of stress parameter, there is decrease in maximum value for thermal wave. In Fig. 6(b), the minima in curves occurs at θ=45° approximately and maxima at θ=65° for tensile stress *a*=0.4 and *a*=0.6 respectively. However, for tensile stress *a*=0.2, maxima at θ=75° for P wave. In Fig. 6(c), the maxima occurs at θ=75°, θ=65° and θ=65° when tensile stress *a*=0.2, *a*=0.4 and *a*=0.6 respectively for SV wave. In Fig. 7(a)-7(b), there is a decrease in amplitude ratio up to θ=45°.

In Fig. 8, the peaks occur at θ=40°, θ=55° and θ=65° when stress *a*=-0.2, *a*=-0.4 and *a*=-0.6 respectively. The nature of the curves is reversing than the previous case of tensile stress. Similarly, in Fig. 9(a)-9(b), the peaks occur at θ=40°, θ=55° and θ=65° when stress *a*=-0.2, *a*=-0.4 and *a*=-0.6 respectively.

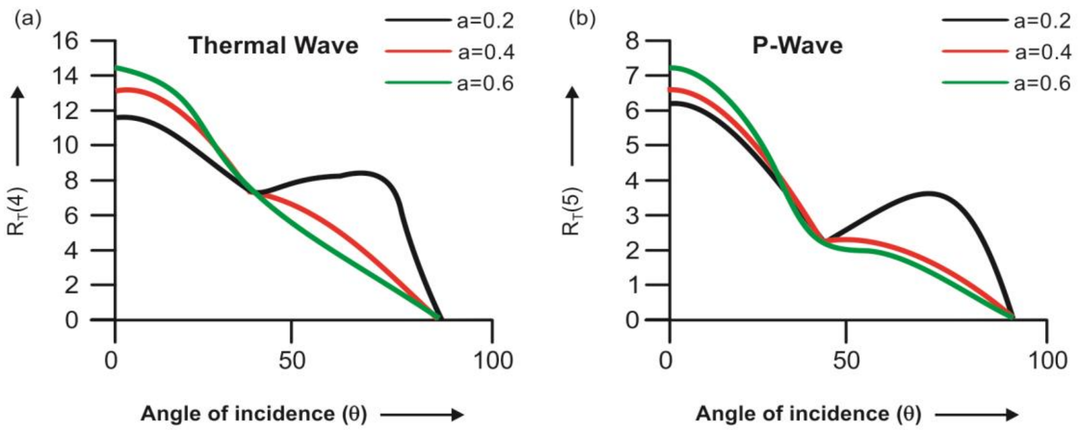

Fig.7 Analysis of amplitude ratio of refracted (a) Thermal wave $|R_T(4)|$ and (b) P wave $|R_T(5)|$ with incident angle under tensile stresses for GL model

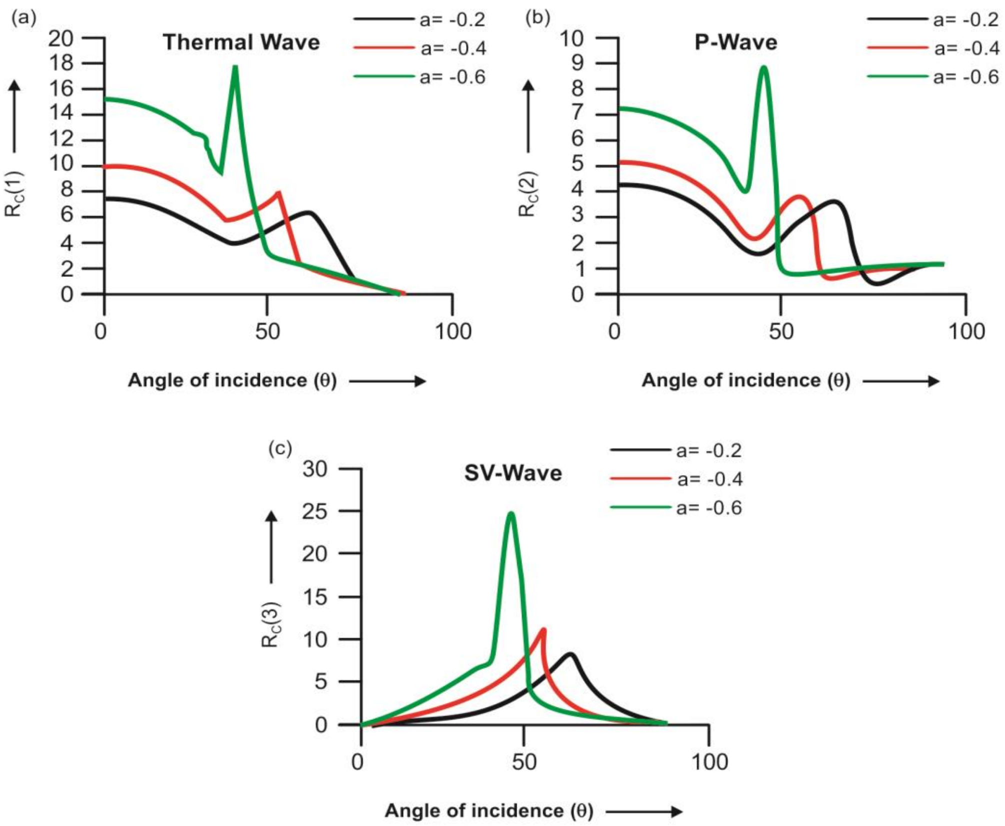

Fig. 8 Analysis of amplitude ratio of reflected (a) Thermal wave $|R_C(1)|$, (b) P wave $|R_C(2)|$ and (c) SV wave $|R_C(3)|$ with incident angle under compressional stresses in GL model

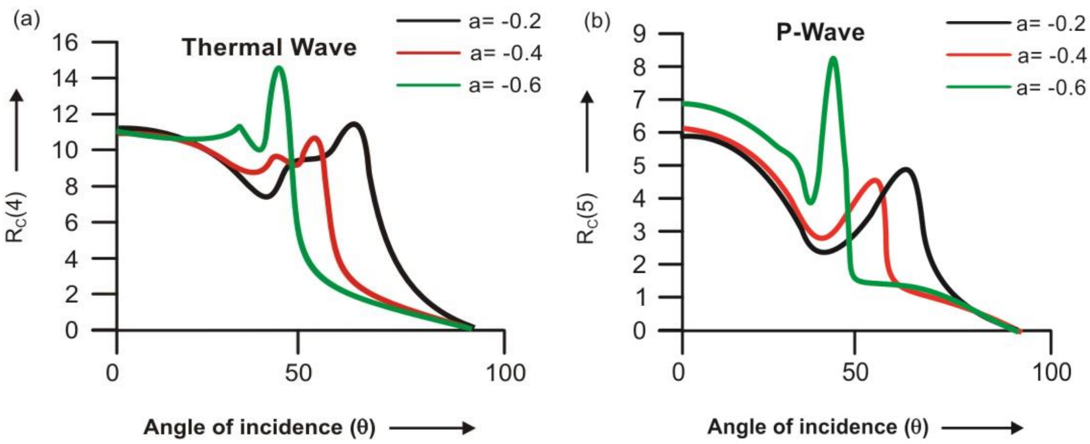

Fig. 9 Analysis of amplitude ratio of refracted (a) Thermal wave and (b) P wave with incident angle unc compressional stresses in GL model

Effect of magnetic parameter

In Figs. 10-13 (when thermal wave is incident), the analysis of amplitude ratios with the incident angle have been compared for different values of magnetic parameters at constant initial stress (tensile and compressional) by taking GL model as sample. In Fig. 10, the analysis of amplitude ratio of reflected (a) Thermal wave $|R_T(1)|$, (b) P wave $|R_T(2)|$ and (c) SV wave $|R_T(3)|$ with incident angle for magneto-thermoelastic wave with tensile stress (a=0.5) at various value of magnetic parameter for incident thermal wave is shown. From Fig. 10, we observe that the amplitude ratios of the reflected thermal waves decrease with increase in incident angle. Also, it is seen that as the magnetic parameter increases, there is a decrease in amplitude ratio. The peak in the amplitude for lower value of magnetic field is observed in all the figures. The amplitude ratios tend to 0 at θ=90° (Fig. 10a-10c). Fig. 11 shows the analysis of amplitude ratio of refracted (a) Thermal wave $|R_T(4)|$ and (b) P wave $|R_T(5)|$ with incident angle under different values of magnetic field with tensile stress (a=0.5) for incident thermal wave. The amplitude ratios of the refracted waves decrease slowly and maximum for lower value of magnetic parameter. The amplitude ratios tend to 0 at θ=90° (Fig. 11a-11b). Fig. 12 shows the analysis of amplitude ratio of reflected (a) Thermal wave $|R_C(1)|$, (b) P wave $|R_C(2)|$ and (c) SV wave $|R_C(3)|$ with incident angle with compressional stress (a=-0.5) at various value of magnetic parameter for incident thermal wave is shown. From Fig. 12, we observe that the amplitude ratios of the reflected thermal waves decrease with increase in incident angle. Also, it is seen that as the magnetic parameter increases, there is an increase in amplitude ratio. The peak in the amplitude for higher value of magnetic field is observed in all the figures. The amplitude ratios tend to 0 at θ=90° (Fig. 12a-12c). Fig. 13 shows the analysis of amplitude ratio of refracted (a) Thermal wave $|R_C(4)|$ and (b) P wave $|R_C(5)|$ with incident angle with compressional stress (a=-0.5) at various value of magnetic parameter for incident thermal wave is shown. From Fig. 13, we observe that the amplitude ratios of the reflected thermal waves decrease with increase in incident angle. The amplitude ratios tend to 0 at θ=90° (Fig. 13a-13b).

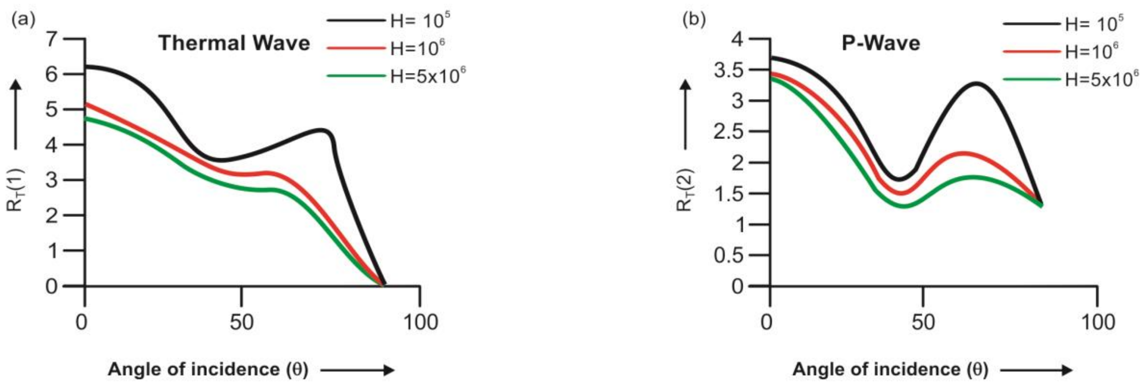

Fig. 10 Analysis of amplitude ratio of reflected (a) Thermal wave $|R_T(1)|$, P wave $|R_T(2)|$ and (c) SV wave $|R_T(3)|$ with incident angle for different magnetic fields when the stress is tensile

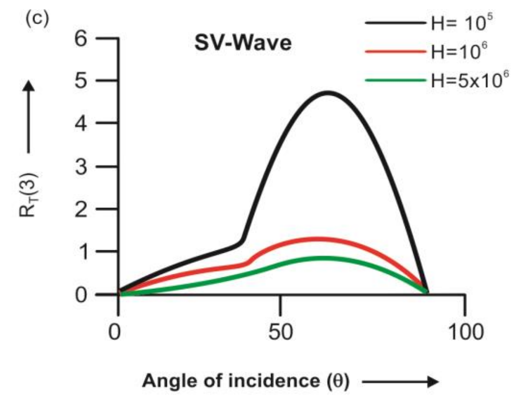

Fig. 10 Continued

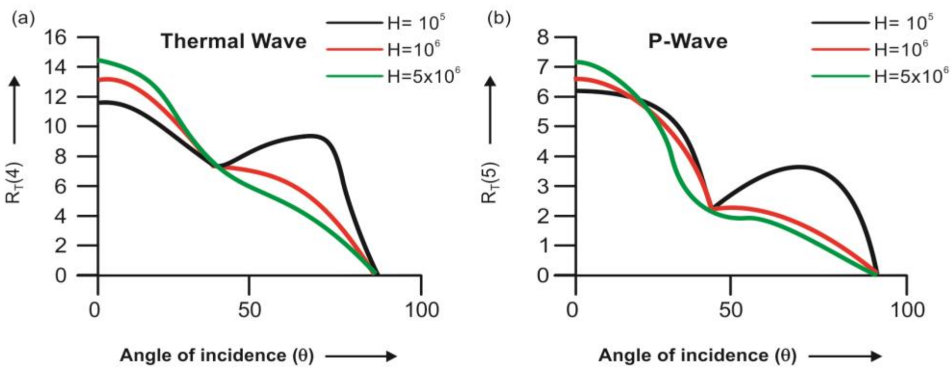

Fig. 11 Analysis of amplitude ratio of refracted (a) Thermal wave $|R_{\mathrm{T}}(4)|$ and (b) P wave $|R_{\mathrm{T}}(5)|$ with incident angle for different magnetic fields when the stress is tensile

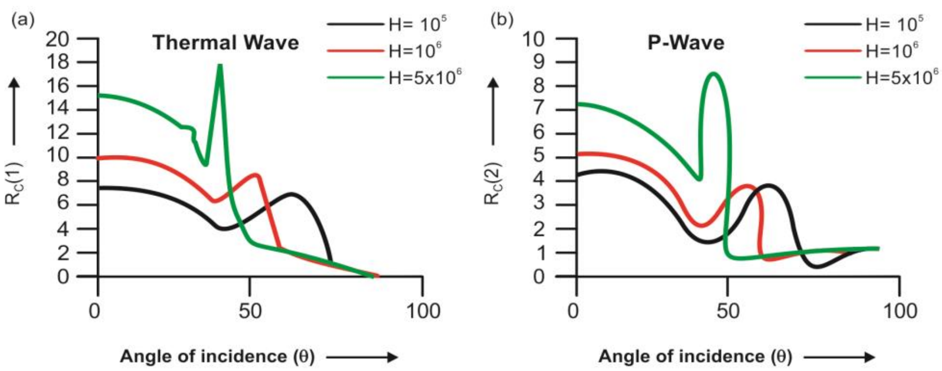

Fig. 12 Analysis of amplitude ratio of reflected (a) Thermal wave $|R_{\mathrm{C}}(1)|$, (b) P wave $|R_{\mathrm{C}}(2)|$ and (c) SV wave $|R_{\mathrm{C}}(3)|$ with incident angle for different magnetic fields when the stress is compressional

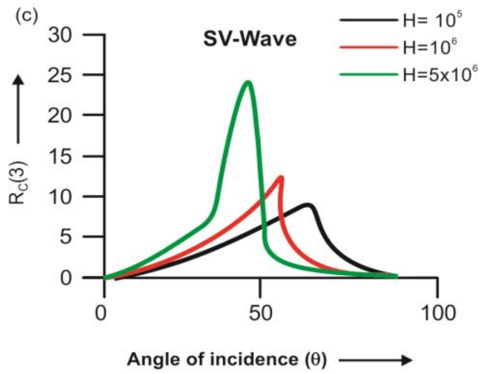

Fig. 12 Continued

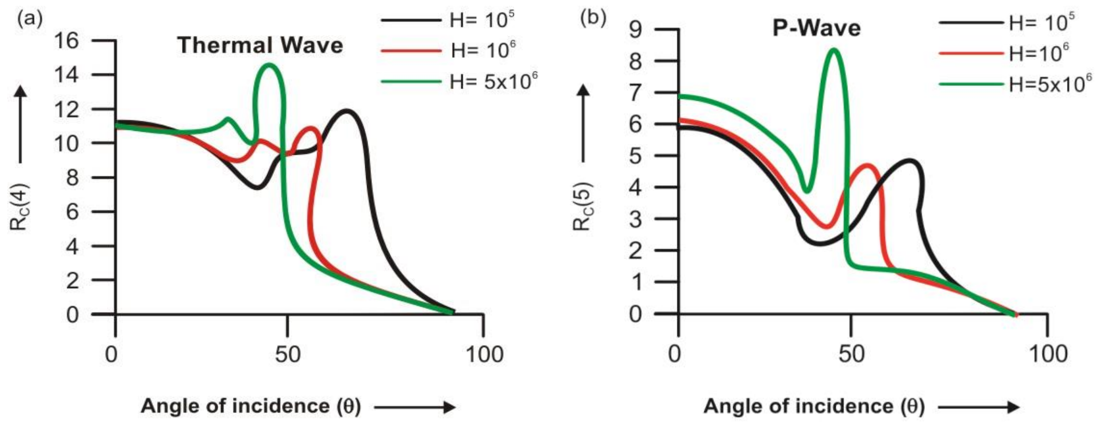

Fig. 13 Analysis of amplitude ratio of refracted (a) Thermal wave $|R_C(4)|$ and (b) P wave $|R_C(5)|$ with incident angle for different magnetic fields when the stress is compressional

7. Conclusions

Comparative studies of reflection and refraction of thermal wave, P wave and SV wave at the interface of water-cadmium in pre-stressed half space with both compressive and tensile stress is made in the three models of thermoelasticity. The problem is reduced to the solution of equations under fixed boundary conditions. The following conclusions can be drawn from the above studies:

(1) It has been observed that the amplitude ratios $|R_i|$ of plane waves depend on the incident angle of the incident wave, stress parameter and magnetic parameter of the medium.

(2) From the above graphs, it is seen that the reflection and refraction or transmission of magneto-thermoelastic waves under initial stress is almost same in LS, GL and CT models of generalized thermoelasticity, but the magnitude of amplitude ratio is slightly different for various values of incident angles and initial hydrostatic stress.

(3) The magnetic field significantly affects the velocities of the waves and reflection and

refraction amplitude.

This investigation is useful for seismologists and geologists to study the effect of magnetic field, temperature and initial stress of earth on different liquid-solid layers present in the earth mantle and crust.

Acknowledgments

The authors are thankful to unknown reviewers for their valuable comments.

References

Biot, M.A. (1965), *Mechanics of Incremental Deformations*, John Wiley and Sons, Inc., New York.

Biot, M.A. (1956), "Thermoelasticity and irreversible thermodynamics", *J. Appl. Phys*., **27**(3), 240.

Chen, J.Y., Chen, H.L. and Pan, E. (2008), "Reflection and transmission coefficients of plane waves in magnetoelectroelastic layered structures", *J. Vib. Acoust.*, **130**(3), 031002.

Dey, S. and Addy, S.K. (1977), "Reflection of plane waves under initial stresses at a free surface", *Int. J. Non Linear Mech.*, **12**(6), 372-381.

Feng, W.J., Jin, J. and E. Pan (2008), "Stoneley (interfacial) waves between two magneto-electroelastic half planes", *Philos. Mag.*, **88**(12), 1801-1810.

Green, A.E. and Lindsay, K.A. (1973), "Thermoelasticity", *J. Elasticity*, **2**(1), 1-7.

Kaur, R. and Sharma, J.N. (2012), "Study of reflection and transmission of thermoelastic plane waves at liquid- solid interface", *J. Int. Academy Phys. Sci.*, **16**(2), 109-116.

Lord, H.W. and Shulman, Y. (1967), "A generalized dynamical theory of thermoelasticity", *J. Mech. Phys. Solid.*, **15**(5), 299-309.

Lotfy, K. (2011), "Transient disturbance in a half-space under generalized magneto-thermoelasticity with a stable internal heat source under three theories", *Multidiscipline Model. Mater. Struct*., **7**(1), 73-90.

Melkumyan, A. (2007), "Twelve shear surface waves guided by clamped/free boundaries in magneto-electro-elastic materials", *Int. J. Solid. Struct.*, **44**(10), 3594-3599.

Othman, M.I.A. and Song, Y. (2008), "Reflection of magneto-thermoelastic waves with two relaxation times and temperature dependent elastic moduli", *Appl. Math. Model.*, **32**(4), 483-500.

Sinha, S.B. and Elsibai, K.A. (1996), "Reflection of thermoelastic waves at a solid half-space with two relaxation times", *J. Therm. Stress.*, **19**(8), 763-777.

Sharma, J.N., Kumar, V. and Chand, D. (2003), "Reflection of generalized thermoelastic waves from the boundary of a half-space", *J. Therm. Stress.*, **26**(10), 925-942.

Singh, M.C. and Chakraborty, N. (2013), "Reflection and refraction of P-, SV- and thermal wave, at an initially stressed solid-liquid interface in generalized thermoelasticity", *Appl. Math. Model.*, **37**(1), 463-475.

Sharma, K. and Bhargava, R.R. (2014), "Propagation of thermoelastic plane waves at an imperfect boundary of thermal conducting viscous liquid/generalized thermoelastic solid", *Afrika Matematika*, **25**(1), 81-102.

Wu, X.H., Shen, Y.P. and Sun, Q. (2007), "Lamb wave propagation in magnetoelectroelastic plates", *Appl. Acoust.*, **68**(10), 1224-1240.

Zhang, R. (2013), "Reflection and refraction of plane waves at the interface between magnetoelectroelastic and liquid media", *Theo. Appl. Mech*., **40**(3), 427-439.

CC

Appendix

$$c_1^2 = \frac{(\lambda + 2\mu + \mu_e \mathrm{H}_0^2 + P)}{\rho} = \frac{2\mu}{\rho}\left(1 + a + \frac{\lambda}{2\mu} + \frac{\mu_e \mathrm{H}_0^2}{2\mu}\right),\ c_1'^2 = \frac{(\lambda' + \mu_e' \mathrm{H}_0'^2)}{\rho'},$$

$$c_2^2 = \frac{\left(\mu - \frac{P}{2}\right)}{\rho} = \frac{\mu(1-a)}{\rho},\ \beta = \frac{P}{\rho c_2^2} = \frac{2a}{1-a},\ c_3^2 = \frac{\mathrm{K}}{\rho c_v},\ c_3'^2 = \frac{\mathrm{K}'}{\rho' c_v'},\ \tau = \frac{3\mathrm{K}}{\rho c_v c_1^2},$$

$$\tau' = \frac{3\mathrm{K}'}{\rho' c_v' c_1'^2}$$

Nomenclature

λ, μ	Lame's constants
ρ	density
σ	Poisson's ratio
c_v	specific heat at constant strain
s_{ij}	components of stress tensor
T	absolute temperature
T_0	reference temperature chosen so that $\lvert \mathrm{T} - \mathrm{T}_0 / \mathrm{T}_0 \rvert \ll 1$
P	Initial pressure ($s_{yy} - s_{xx}$)
e_{ij}	components of strain tensor
K	thermal conductivity
J	current density vector
μ_e	$1/[2(1+\sigma)]$ magnetic permeability
ε_e	electric permittivity
H	initial uniform magnetic intensity vector
h	induced magnetic field
H_0	magnetic field component
E	induced electric field vector
D	electric displacement vector
B	magnetic displacement vector
F	Lorentz force
δ_{ij}	Kronecker delta
τ_{T}	thermoelastic coupling constant
u_i	components of displacement vector

τ_0, τ	relaxation times
t	time
e	cubical dilatation
Ω	$1/2(\partial v/\partial x - \partial u/\partial y)$ rotational component
α_t	coefficient of linear thermal expansion
γ	$(3\lambda + 2\mu)\alpha_t$
k	wave number
ω	angular frequency
c	ω / k
c_1^2	$(\lambda + 2\mu + \mu_e \mathrm{H}_0^2 + P)/\rho$
c_2^2	$\left(\mu - P/2\right)/\rho$
c_3^2	$\mathrm{K}/\rho c_v$
c^2	$1/\mu_e \varepsilon_e$ light speed squared